ISSN 1070-3284, Russian Journal of Coordination Chemistry, 2018, Vol. 44, No. 2, pp. 147–154. © Pleiades Publishing, Ltd., 2018.
Original Russian Text © M.Yu. Afonin, T.S. Sukhikh, A.Yu. Konokhova, S.N. Konchenko, 2018, published in Koordinatsionnaya Khimiya, 2018, Vol. 44, No. 1, pp. 58–64.

Reactions of Chalcogenide β-Diiminate Nickel Complexes with Samarium Bis(pentamethylcyclopentadienide)

M. Yu. Afonin[a, *], T. S. Sukhikh[a, b], A. Yu. Konokhova[a, b], and S. N. Konchenko[a, b]

[a] *Nikolaev Institute of Inorganic Chemistry, Siberian Branch, Russian Academy of Sciences, Novosibirsk, 630090 Russia*
[b] *Novosibirsk State University, ul. Pirogova 2, Novosibirsk, 630090 Russia*
**e-mail: afonin@niic.nsc.ru*

Received June 24, 2017

Abstract—The reactions of $[(L^{iPr}Ni)_2(\mu\text{-}\eta^2\text{:}\eta^2\text{-}S_4)]$ (**I**) and $[(L^{iPr}Ni)_2(\mu\text{-}\eta^2\text{:}\eta^2\text{-}Se_2)]$ (**II**) (L^{iPr} = $CH[C(Me)N(2,6\text{-}{}^{i}Pr_2C_6H_3)]_2$) with decamethylsamarocene $[Sm(Cp^*)_2(Thf)_2]$ ($Cp^* = \eta^5\text{-}C_5Me_5$) are studied. It is assumed that the reactions afford hetero-*d*/*f*-metal complexes. However, these complexes are not observed but the transfer of chalcogens from Ni to Sm and the formation of $[(Sm(Cp^*)_2(Thf))_2(\mu\text{-}S)]$ (**III**) and $[(Sm(Cp^*)_2(Thf))_2(\mu\text{-}Se)]$ (**IV**) occur. The second reaction products are $[(L^{iPr}Ni)_2(\mu\text{-}\eta^2\text{:}\eta^2\text{-}S_2)]$ (**V**) in the case of sulfur and $[(L^{iPr}Ni^{I})_2(\mu\text{-}\eta^6\text{:}\eta^6\text{-}C_7H_8)_2]$ (**VI**) in the case of selenium. All reaction products have been described previously, but compounds **III** and **V** are isolated as new crystalline phase, the structures of which are determined by X-ray diffraction analysis (CIF files CCDC nos. 1559045 (**V**) and 1559046 (**III**)).

Keywords: samarium, nickel, chalcogenide complexes, crystal structure
DOI: 10.1134/S107032841802001X

INTRODUCTION

Molecular complexes of lanthanides (Ln) bearing the Ln–Q bond (Q = S, Se, Te) are scarce and poorly studied. They are often named "unusual" or "nontraditional," since these complexes combine in one molecule a hard acid (Ln^{3+}) and a soft base (chalcogenide ligand), which leads to the manifestation of unusual physical and chemical properties [1–3]. For example, the results obtained by studying the luminescence of the polynuclear chalcogenide complexes of lanthanides in the near-IR range showed that the introduction of the anionic chalcogen-containing ligands into the coordination sphere of Ln^{3+} substantially stabilized the excited state and considerably increased the quantum yield [4–7]. In addition, the lanthanide chalcogenide complexes rich in unpaired electrons are interesting from the viewpoint of magnetic properties. For instance, the dysprosium complexes with the bridging chalcogenolate ligands exhibit the properties of single-molecule magnets [8, 9].

The experimental material available to the present time suggests that the most interesting properties can be expected for the polynuclear complexes among which polychalcogenide and heteromagnetic complexes containing different Ln or simultaneously Ln and *d*-element in one molecule attract special attention. The development of methods for the synthesis of these compounds is urgent.

We have previously developed an original approach to the synthesis of one more class of "nontraditional" lanthanide compounds, namely, polypnictide hetero-Ln/*d*-metallic polynuclear complexes, which are synthesized by the reduction of the polypnictide complexes of *d*-metals with the Ln(II) compounds [10–14]. The same approach was successfully used for the synthesis of $[Fe_6Ln_2(\mu_3\text{-}S)_6(\mu,\eta^2\text{-}CO)_4(CO)_8(Cp^*)_4]$ by the reaction of $[Fe_2(\mu\text{-}\eta^2\text{:}\eta^2\text{-}S_2)(CO)_6]$ with $[Ln(Cp^*)_2(Thf)_2]$ (Ln = Sm, Yb; Thf is tetrahydrofuran) [15]. However, this is the single example of the accomplishment of the "reduction" approach to chalcogenide hetero-Ln/*d*-metallic complexes so far. This work is devoted to the further development of this approach.

The purpose of the work is to study the reactions of samarocene with the polychalcogenide nickel complexes $[(L^{iPr}Ni)_2(\mu\text{-}\eta^2\text{:}\eta^2\text{-}S_4)]$ (**I**) and $[(L^{iPr}Ni)_2(\mu\text{-}\eta^2\text{:}\eta^2\text{-}Se_2)]$ (**II**), where L^{iPr} is $CH[CMeN(2,6\text{-}{}^{i}Pr_2C_6H_3)]_2$, and to reveal the possibility of obtaining chalcogenide Sm/Ni complexes.

EXPERIMENTAL

The reactions were carried out in evacuated sealed ampules. The substances were loaded into a box filled with argon. The starting complexes **I** and **II** and $[Sm(Cp^*)_2(Thf)_2]$ were obtained according to

described procedures ([16], [17], and [18], respectively). Toluene was distilled over sodium and kept in an evacuated vessel over a potassium–sodium alloy. IR spectra were recorded on an FT-801 spectrophotometer (Simex) in KBr pellets.

Reaction of complex I with $[Sm(Cp^*)_2(Thf)_2]$. A two-section ampule was used, whose sections (A and B) were arranged at an angle of 90°. The solid reactants **I** (0.027 g, 0.025 mmol) and $[Sm(Cp^*)_2(Thf)_2]$ (0.057 g, 0.1 mmol) were loaded into section A of the ampule in the box filled with argon. The ampule was attached to a vacuum condensation apparatus. Toluene (~15 mL) was condensed into the same section cooled with liquid nitrogen. Then the ampule was sealed off. The reaction mixture was stirred for 3 days at room temperature. The obtained solution was decanted to section B, after which section A was placed in a vessel with cold water, while the solution in section B was of room temperature. In approximately one weak, the slow concentration of the solution by the re-evaporation of the solvent to section A resulted in the formation of a mixture of yellow crystals of the $[(Sm(Cp^*)_2(Thf))_2(\mu\text{-}S)]$ complex (**III**) and red crystals of the $[(L^{iPr}Ni)_2(\mu\text{-}\eta^2\text{:}\eta^2\text{-}S_2)]$ complex (**V**). The mother liquor was decanted to section A, and the crystals were washed with a minor amount of toluene using the backward condensation of a portion of the solvent to section B and repeated decantation. The obtained crystalline substance was dried by the cooling of section A with liquid nitrogen, after which section B was sealed off and placed in a box with argon, where section B was opened and the crystals of compounds **III** and **V** were taken out. The overall weight of the crystals was 0.031 g. The crystalline samples were separated manually to record IR spectra.

The reaction of compound V with $[Sm(Cp^*)_2(Thf)_2]$ was carried out similarly to that presented above starting from complex **II** (0.020 g, 0.018 mmol) and $[Sm(Cp^*)_2(Thf)_2]$ (0.040 g, 0.07 mmol). The overall weight of the yellow crystals of complex $[(Sm(Cp^*)_2(Thf))_2(\mu\text{-}Se)]$ (**IV**) and the red crystals of complex $[(L^{iPr}Ni^I)_2(\mu\text{-}\eta^6\text{:}\eta^6\text{-}C_7H_8)_2]$ (**VI**) was 0.028 g. The crystalline samples were separated manually to record IR spectra.

X-ray diffraction analyses of complexes **III** and **V** were conducted using a standard procedure on a Bruker Apex DUO automated four-circle diffractometer equipped with a two-coordinated CCD detector (MoK_α radiation, $\lambda = 0.71073$ Å, graphite monochromator) at 150 K. Reflection intensities were measured using the φ and ω scan modes for narrow (0.5°) frames. An absorption correction was applied by the SADABS program [19]. The structures were solved by a direct method and refined by full-matrix least squares in the anisotropic (for non-hydrogen atoms) approximation using the SHELXTL program package [20, 21] and the Olex2 program shell [22]. The crystallographic data and the experimental and refinement details for compounds **III** and **V** are presented in Table 1. Hydrogen atoms were localized geometrically and refined in the rigid body approximation.

The cell parameters for the single crystals of compounds **IV** ($a = 10.864(4)$, $b = 14.958(3)$, $c = 32.816(6)$ Å, $\beta = 95.995(3)°$, $V = 5303.67(6)$ Å^3) and **VI** ($a = 10.738(2)$, $b = 19.709(3)$, $c = 14.082(2)$ Å, $\beta = 94.7513(10)°$, $V = 2970.02(9)$ Å^3) determined at 150 K are close to those for the structures of compounds $[(Sm(Cp^*)_2(Thf))_2(\mu\text{-}Se)]$ [23] and $[(L^{iPr}Ni^I)_2(\mu\text{-}\eta^6\text{:}\eta^6\text{-}C_7H_8)_2]$ [24].

The X-ray diffraction data for the structures of compounds **III** and **V** were deposited with the Cambridge Crystallographic Data Centre (CIF files CCDC nos. 1559045 (**V**) and 1559046 (**III**); deposit@ccdc.cam.ac.uk or http://www.ccdc.cam.ac.uk/data_request/cif) and are available from the authors.

RESULTS AND DISCUSSION

Compounds **I** (Scheme 1) and **II** (Scheme 2) obtained by the treatment of the toluene Ni(I) complex (**VI**) with the corresponding chalcogen [17, 18] a priori look like convenient substrates for the synthesis of the heterometallic derivatives in the reactions with the Sm(II) compounds. First, since they contain the tetra- and dichalcogenide ligands and nickel in the oxidation state +2, it is doubtless that compounds **I** and **II** would act as oxidants with respect to Sm(II). Second, the formation of anionic complexes with nucleophilic centers (chalcogen atoms capable of coordinating to Sm(III) in the absence of other nucleophilic species in the solution) should be expected, because the most probable result of reduction would be the cleavage of the Q–Q bond (Q = S, Se). Third, the presence of the bulky ligand L^{iPr} strongly bound to the nickel atom should prevent the formation of polymeric forms and/or the condensed solid phases, for example, of nickel sulfide. One could expect a priori the result similar to those observed in the reactions of $[Fe_2(\mu\text{-}\eta^2\text{:}\eta^2\text{-}S_2)(CO)_6]$ with $[Ln(Cp^*)_2(Thf)_2]$ (Ln = Sm, Yb) leading to the formation of $[Fe_6Ln_2(\mu_3\text{-}S)_6(\mu,\eta^2\text{-}CO)_4(CO)_8(Cp^*)_4]$ [15].

To check this hypothesis, we studied the reactions of compounds **I** and **II** with $[Sm(Cp^*)_2(Thf)_2]$ at different ratios of the reactants. It turned out that the sets of reaction products were independent of the reactant ratio. In the case of an excess of one of them, this reactant remains unreacted. The ratio **I** (or **II**) : $[Sm(Cp^*)_2(Thf)_2] = 1 : 4$ is optimum from the viewpoint of the maximum yield of the products.

The reaction of compound **I** with $[Sm(Cp^*)_2(Thf)_2]$ (Scheme 1) affords a mixture of yellow and red crystals. It is established by the single-crystal X-ray diffraction analysis method that

Table 1. Crystallographic data and results of structure refinement for complexes **III** and **V**

Parameter	Value	
	III	**V**
Empirical formula	$C_{48}H_{76}O_2SSm_2$	$C_{58}H_{82}N_4S_2Ni_2$
FW	1017.84	1016.81
Crystal system	$P\bar{1}$	$P2/n$
Space group	Triclinic	Monoclinic
a, Å	10.6211(4)	23.297(2)
b, Å	15.4734(6)	10.6623(10)
c, Å	15.7685(7)	23.715(2)
α, deg	65.7310(10)	90
β, deg	87.0980(10)	107.948(3)
γ, deg	81.3380(10)	90
V, Å^3	2335.32(16)	5604.2(9)
Z	2	4
ρ_{calc}, g cm^{-3}	1.447	1.205
μ, mm^{-1}	2.569	0.785
F(000)	1040	2184
Crystal size, mm	0.3 × 0.2 × 0.05	0.45 × 0.2 × 0.08
Range of data collection over θ, deg	1.56–25.74	1.07–25.82
Ranges h, k, l	$-12 \le h \le 12$, $-18 \le k \le 18$, $-19 \le l \le 19$	$-28 \le h \le 28$, $-11 \le k \le 11$, $-28 \le l \le 29$
Number of measured/independent reflections	22597/8877	62140/10763
Number of observed reflections with $I > 2\sigma(I)$	8035	8728
Completeness of data collection, %	99.4	99.6
Transmission max and min	0.7453/0.5840	0.7453/0.6847
Number of refined parameters	498	615
R factor ($I > 2\sigma(I)$)	0.0187	0.0627
R factor (all data)	0.0222	0.0785
GOOF for F^2	1.072	1.111
$\Delta\rho_{max}/\Delta\rho_{min}$, e/Å^{-3}	0.645/–0.411	2.371/–0.830

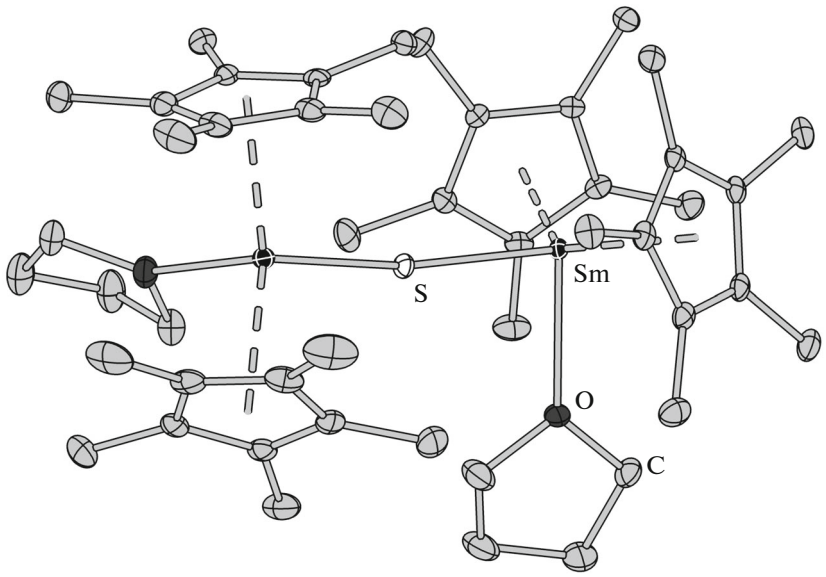

Fig. 1. Structure of complex $[(Sm(Cp^*)_2(Thf))_2(\mu\text{-}S)]$ (**III**). Ellipsoids are presented with 30% probability. Hydrogen atoms are omitted.

the yellow crystals represent $[(Sm(Cp^*)_2(Thf))_2(\mu\text{-}S)]$ (**III**) (Fig. 1), whereas the red crystals are compound $[(L^{iPr}Ni)_2(\mu\text{-}\eta^2\text{:}\eta^2\text{-}S_2)]$ (**V**) (Fig. 2). Both compounds have been known previously, but they were isolated as other crystalline phases: complex **III** was synthesized by the reaction of $[(Sm(Cp^*)_2(Thf))_2]$ with $Ph_3P{=}S$ and isolated in the form of a solvate with toluene (**III** · C_7H_8) [23], whereas complex **V** was obtained by the treatment of compound **I** with triphenylphosphine and isolated in the form of another polymorph, namely, **V'** [16]. The structures of the isolated solid phases and their distinctions from the earlier described structures are discussed below.

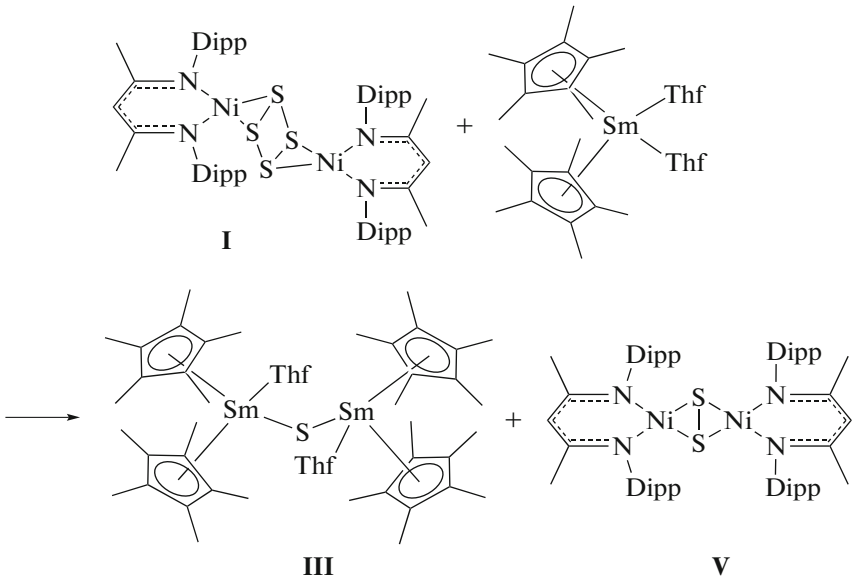

Scheme 1.

The results of the reaction of complex **I** with $[Sm(Cp^*)_2(Thf)_2]$ indicate that, in this case, the reduction of the tetrasulfide ligand occurs in fact, but does not result in a heterometallic complex. "Excessive" sulfur is detached, and decamethylsamarocenium sulfide **III** is formed. The nickel complex loses two of four sulfur atoms, and the remaining sulfur atoms form a disulfide bridge between the nickel

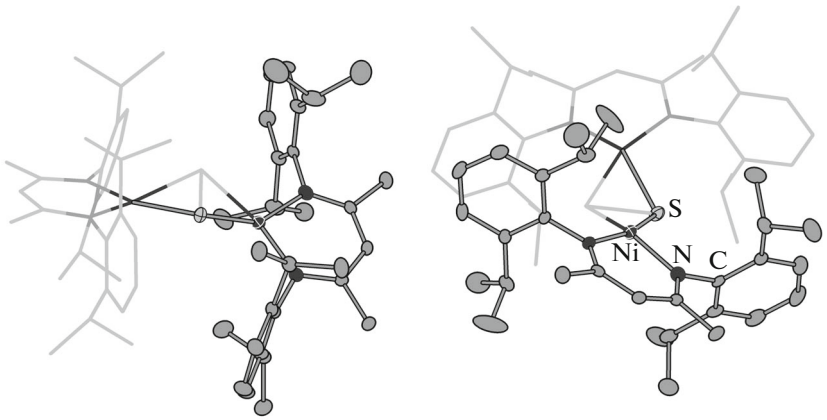

Fig. 2. Structure of complex $[(L^{iPr}Ni)_2(\mu\text{-}\eta^2\text{:}\eta^2\text{-}S_2)]$ (**V**). Ellipsoids are presented with 30% probability. Crystallographically equivalent fragments are shown in the ball-and-stick model. Hydrogen atoms are omitted.

atoms. The oxidation state of nickel remains unchanged.

Unlike compound **I**, complex **II** containing the diselenide bridging ligand (Scheme 2) reacts with $[(Sm(Cp^*)_2(Thf))_2]$ under the same conditions, leading to the reduction of the diselenide ligand to the selenide ligand and to the reduction of the Ni(II) ion to Ni(I).

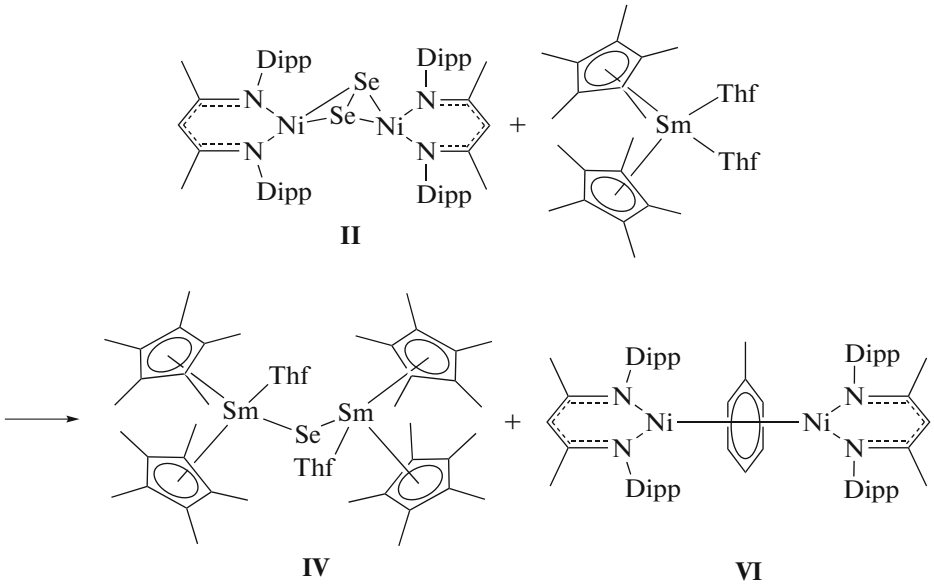

Scheme 2.

As in the case of sulfur, a mixture of yellow and red crystals was isolated and identified by the crystal cell parameters (see Experimental) and the coincidence of the IR spectra with those of the authentic samples of compounds **IV** and **VI**, respectively. Compound **IV** was earlier obtained by the reaction of $[(Sm(Cp^*)_2(Thf))_2]$ with Se [23], whereas complex **VI** was synthesized by the reduction of $[L^{iPr}Ni(\mu\text{-}Br)_2Li(Thf)]_2$ with a K/Na alloy in toluene [24].

The structures of the crystalline phases of compounds **III** and **V** were established by X-ray diffraction analysis for single-crystal samples selected from a mixture of the crystals formed during the slow evaporation of the reaction solution.

The crystalline phase of complex **III** isolated by us is established to contain molecules of the complex, whose geometry is almost identical to that of compound $\mathbf{III \cdot C_7H_8}$ [23] (Table 2). This indicates its relative spatial rigidity, although a certain mobility of the coordination sphere could be expected for the lanthanide complexes. Both crystallographically nonequivalent Sm atoms in compound **III** exist in the same environments of the carbon atoms of two Cp* ligands, the

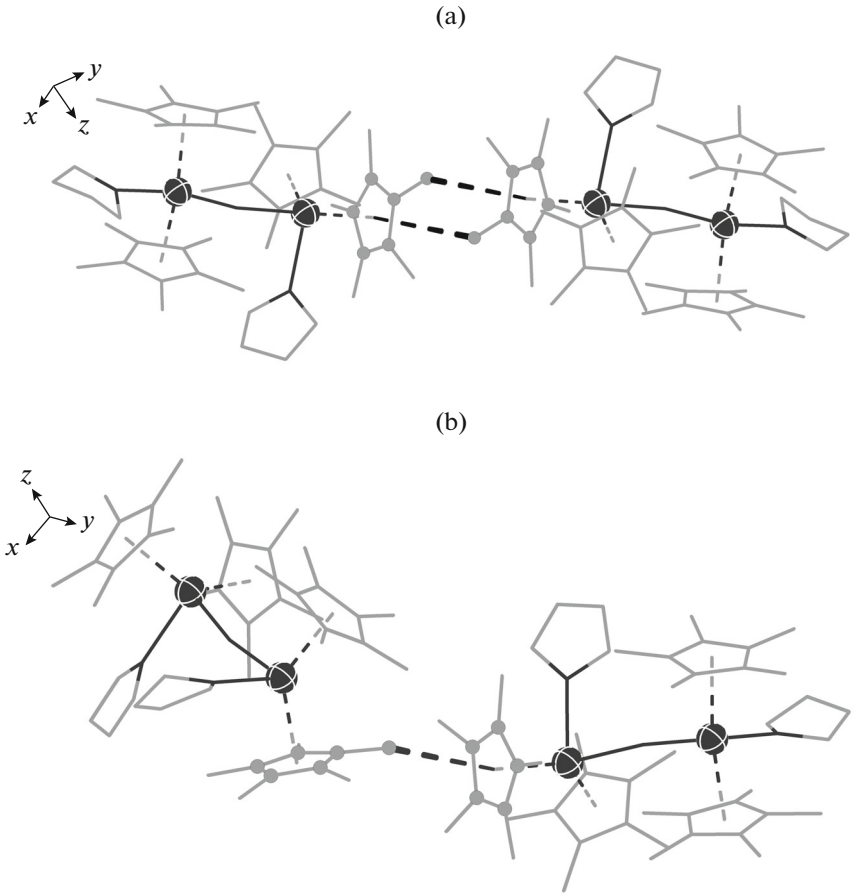

Fig. 3. Packing fragments for compounds (a) [(Sm(Cp*)$_2$(Thf))$_2$(μ-S)] (**III**) and (b) **III** · C_7H_8 (C–H···π contacts are shown by solid lines).

oxygen atom of tetrahydrofuran, and the S atom. According to the CCDC data, the corresponding bond lengths lie in the expected range. The SmSSm angles somewhat deviate from 180°, which is mainly observed in a yet few examples of similar complexes with the {Ln–S–Ln} fragment [25–27]. The distinctions in the crystal packings of compounds **III** and **III** · C_7H_8 are observed because of the absence of solvate molecules in **III** and the presence of those in **III** · C_7H_8. In the case of complex **III**, the molecules of the complex are mutually parallel, since crystallographically they are linked only by the inversion center and translation. In

Table 2. Selected interatomic distances and bond angles in complexes **III** and **V** and in the crystalline phases of compounds **III** · C_7H_8 [13] and **V'** [14]

Parameter	Value			
	III	**III** · C_7H_8	**V**	**V'**
M–S, Å	2.6650(6), 2.6821(6)	2.6647(13), 2.6626(12)	2.2083(12), 2.2085(13), 2.2067(13), 2.2286(14)	2.1934(10), 2.2203(10), 2.1989(11), 2.2054(10)
MSM, deg	169.18(2)	169.95(5)	110.40(5), 111.67(6)	108.48(4), 109.70(4)
X–M···M–X (X = O, N), deg	73.67(6)	72.54(11)	29.1(2), 35.2(2)*	34.7(1), 39.8(2)*
M···M, Å	5.3235(5)	5.3069(13)	3.6268(7), 3.6701(8)	3.5913(6)
Centroid C5–Sm–centroid C5, deg	131.877(11), 130.773(11)	132.54(2), 132.36(2)		

* The smallest angle.

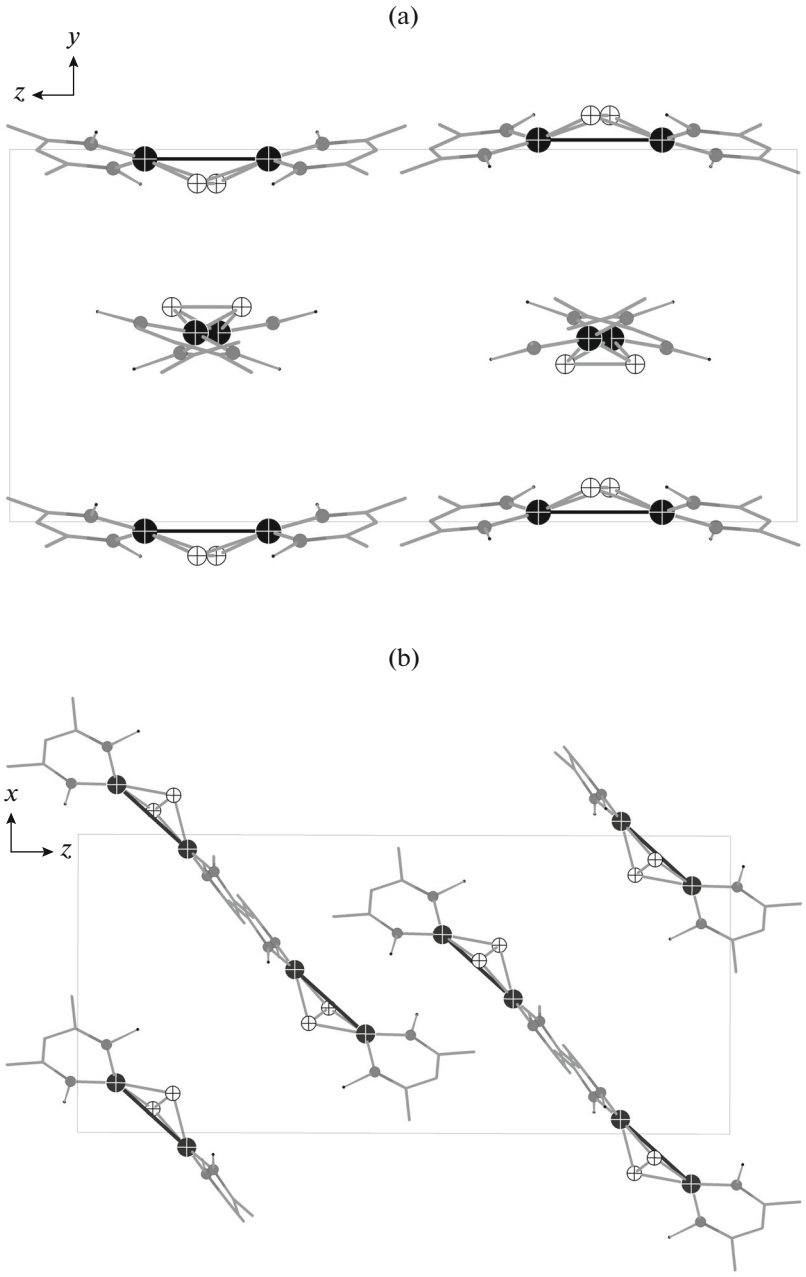

Fig. 4. Packing fragments for compounds (a) $[(L^{iPr}Ni)_2(\mu\text{-}\eta^2\text{:}\eta^2\text{-}S_2)]$ (**V**) and (b) **V'**. The phenyl rings of the ligands are omitted.

the case of compound **III** · $\mathbf{C_7H_8}$, the adjacent molecules are arranged at an angle of 38.2° to each other (the angle between the lines connecting the Sm atoms in the molecule) due to the 2_1 axis and the *c* plane. The relative arrangements of the Cp* ligands in the adjacent molecules also differ. In the phase of compound **III**, the nearest Cp* ligands are parallel. The distance between the C atom of the methyl group and the center of the adjacent ring (Fig. 3) is 3.582(6) Å, indicating the presence of pair intermolecular contacts C–H···π [28]. Similar ordinary contacts are also observed in the phase of **III** · $\mathbf{C_7H_8}$ (the corresponding distance is 3.536(6) Å). However, the planes of the rings of the Cp* ligands are not mutually parallel but lie at an angle of 76.2° to each other. This is related, most likely, to the solvate toluene molecules also interacting similarly due to the $(C_6H_5)CH_3\cdots\pi$(Cp*) contacts (C···C 3.464(8) Å).

The phase of compound **V** contains two crystallographically independent molecules with the C_2 symmetry (Fig. 2). In these molecules, the coordination mode is a distorted square. The molecules in the phase of **V'** have the C_1 symmetry due to minor quantitative differences in the bond lengths and angles (Table 2). In

the case of compound **V**, the $\{Ni_2S_2\}$ fragments are somewhat more planar than those in compound **V'**, which appears as smaller NiSNi angles (by 4.5°) and shorter Ni···Ni distances (by 0.03 and 0.08 Å) in **V'**. The packings of the complex are different (Fig. 4). The molecules in **V'** are oriented along one direction (the angle between the lines connecting the Ni atoms in the molecule is 0° and 9.6°). The layers inside which the molecules are oriented along one direction can be distinguished in the phase of compound **V**, whereas in the adjacent layers the molecules are arranged nearly at the right angle (85.6°) to each other. It can be assumed that different phases are formed because of different crystallization conditions: slow evaporation in the case of **V** and cooling of the solution in the case of **V'**.

Thus, we found that no heterometallic complexes were formed in the studied reactions of complexes **I** and **II** with decamethylsamarocene $[Sm(Cp^*)_2(Thf)_2]$. The result of the reactions is the reduction of the polychalcogenide ligand. In the case of selenium, the reduction is also accompanied by the reduction of Ni(II) to Ni(I). In the cases of both sulfur and selenium, the binuclear homometallic samarium complexes $[(Sm(Cp^*)_2(Thf))_2(\mu\text{-}Q)]$ (Q = S, Se) are formed.

ACKNOWLEDGMENTS

This work was supported by the Russian Science Foundation, grant no. 16-13-10294.

REFERENCES

1. Brennan, J., in *The Rare Earth Elements: Fundamentals and Applications*, Atwood, J., Ed., 2012, p. 215.
2. Li, H.X., Zhu, Y.J., Cheng, M.L., et al., *Coord. Chem. Rev.*, 2006, vol. 250, p. 2059.
3. Nief, F., *Coord. Chem. Rev.*, 1998, vols. 178–180, p. 13.
4. Moore, B.F., Kumar, G.A., Tan, M., et al, *J. Am. Chem. Soc.*, 2011, vol. 132, p. 373.
5. Kornienko, A., Moore, B.F., Kumar, G.A., et al., *Inorg. Chem.*, 2011, vol. 50, p. 9184.
6. Banerjee, S., Kumar, A., Emge, T., et al., *Chem. Mater.*, 2008, vol. 20, p. 4367.
7. Kumar, G.A., Riman, R.E., Diaz Torres, L.A., et al., *Chem. Mater.*, 2007, vol. 19, p. 2937.
8. Layfield, R.A., *Organometallics*, 2014, vol. 33, p. 1084.
9. Pugh, T., Vieru, V., Chibotaru, L., and Layfield, R.A., *Chem. Sci.*, 2016, vol. 7, p. 2128.
10. Konchenko, S.N., Scheer, M., Roesky, P.W., et al., *Angew. Chem., Int. Ed. Engl.*, 2016, vol. 55, p. 1557.
11. Arleth, N., Gamer, M.T., Köppe, R., Roesky, P.W., et al., *Chem. Sci.*, 2015, vol. 6, p. 7179.
12. Li, T., Wiecko, J., Konchenko, S.N., et al., *Angew. Chem., Int. Ed. Engl.*, 2011, vol. 50, p. 9491.
13. Li, T., Gamer, M.T., Konchenko, S.N., et al., *Inorg. Chem.*, 2013, vol. 54, p. 14231.
14. Li, T., Gamer, M.T., Konchenko, S.N., et al., *Chem. Commun.*, 2013, vol. 49, p. 2183.
15. Konchenko, S.N., Sanden, T., Pushkarevsky, N.A., et al., *Chem.-Eur. J.*, 2010, vol. 16, p. 14278.
16. Yao, S., Milsmann, C., Bill, E., et al., *J. Am. Chem. Soc.*, 2008, vol. 130, p. 13536.
17. Yao, S., Xiong, Y., and Zhang, X., *Angew. Chem., Int. Ed. Engl.*, 2009, vol. 48, p. 4551.
18. Evans, W.J., Bloom, I., Hunter, W.E., and Atwood, J.L., *J. Am. Chem. Soc.*, 1981, vol. 103, p. 6507.
19. *APEX2 (version 2.0), SAINT (version 8.18c), SADABS (version 2.11)*, Madison (WI, USA): Bruker AXS Inc., 2000–2012.
20. Sheldrick, G.M., *Acta Crystalllogr., Sect. A: Found. Crystallogr.*, 2008, vol. 64, p. 112.
21. Sheldrick, G.M., *Acta Crystalllogr., Sect. C: Struct. Chem.*, 2015, vol. 71, p. 3.
22. Dolomanov, O.V., Bourhis, L.J., Gildea, R.J., et al., *Appl. Crystalllogr.*, 2009, vol. 42, p. 339.
23. Evans, W.J., Rabe, G.W., Ziller, J.W., and Doedens, R.J., *Inorg. Chem.*, 1994, vol. 33, p. 2719.
24. Bai, G., Wei, P., and Stephan, D.W., *Organometallics*, 2005, vol. 24, p. 5901.
25. Maria, L., Soares, M., Santos, I.C., et al., *Dalton Trans.*, 2016, vol. 45, p. 3778.
26. Fieser, M.E., Johnson, C.W., Bates, J.E., et al., *Organometallics*, 2015, vol. 34, p. 4387.
27. Turcitu, D., Nief, F., and Ricard, L., *Chem.-Eur. J.*, 2003, vol. 9, p. 4916.
28. Janiak, C., *Dalton Trans.*, 2000, p. 3885.

Translated by E. Yablonskaya